be in a trans-trans type such as B.

Now a question arises as to why the anion of *m*-PBPM prefers a trans-trans conformation. This question of the difference in the molecular structure favored by the neutral species and by its anion is considered to be a crucial problem in spin chemistry. As far as we known,[13,14b,27] neutral high-spin molecules of a linear molecular struture often undergo thermally stimulated conformational changes such as phenyl ring flips,[13,14b] when generated by UV photolysis in solid, *without* the change in the spin multiplicity. As for the monoanion of *m*-PBPM formed by photolytic denitrogenation of the monoanion of 1,3-BDB, there may be chances in molecular structural changes during the whole series of reactions starting from the electron attachment to the parent 1,3-BDB. However, since there is little experimental information on the molecular structure of each stage of the reactions,[34] arguments on the spin-conversion process in relation to molecular structures are prohibitive at the moment. Appropriate molecular orbital calculations for charged high-spin molecules may shed light on this problem. A project along this line is now under way.

(34) The spin conversion process from singlet-state 1,3-BDB to quintet-state *m*-PBPM has been studied by time-resolved picosecond laser optical spectroscopy: T. Takui and K. Itoh, unpublished work.

## Conclusion

From the present work it was determined that the ground state of the monoanion of *m*-PBPM is quartet. A theory suggesting the possibility of the reversal of the order of high- and low-spin states upon charging[22] is not substantiated in this system. From the $^1$H-ENDOR measurements it is concluded that the excess electron resides on the nonbonding $\pi$-orbital. This result is compatible with the ESR measurement of the $^{13}$C substituted isotopomer. The molecular conformation of the anion is suggested to be of a trans-trans type.

**Acknowledgment.** The Kyoto group is indebted to Professor Takashi Kawamura for this generosity in allowing us to use his ESR equipment. The Osaka group thanks both the Computer Center, Institute for Molecular Science, Okazaki National Research Institutes for the use of the HITAC M68OH computer and the Computer Center, Osaka City University. Spectral simulations were also carried out at the Data Processing Center of Kyoto University. The study was partially supported by Grants-in-Aid for Scientific Research on priority Areas (Grant Nos. 02205070, 02205102, and 04242103) and Grant-in-Aid for General Scientific Research (Grant Nos. 02453014 and 03640429) of the Ministry of Education, Science, and Culture in Japan.

# Using Saturation-Recovery EPR To Measure Exchange Couplings in Proteins: Application to Ribonucleotide Reductase

**Donald J. Hirsh,[†] Warren F. Beck,[†,‡] John B. Lynch,[§] Lawrence Que, Jr.,[§] and Gary W. Brudvig*,[†]**

*Contribution from the Departments of Chemistry, Yale University, 225 Prospect Street, New Haven, Connecticut 06511, and University of Minnesota, 207 Pleasant Street, S.E., Minneapolis, Minnesota 55455.* *Received February 28, 1992*

**Abstract:** The stable tyrosine radical of ribonucleotide reductase (RNR) from *Escherichia coli*, Tyr 122 of the B2 subunit, exhibits single-exponential spin-lattice relaxation kinetics for $T \leq 16$ K and nonexponential spin-lattice relaxation kinetics at higher temperatures. Saturation-recovery transients of the tyrosine radical are analyzed using a model developed to treat the interaction of two paramagnets in a rigid lattice at a fixed distance apart but with a randon orientation in the static magnetic field. The model describes the spin-lattice relaxation of a radical in proximity to another paramagnetic site in terms of two isotropic or "scalar" rate constants and an orientation-dependent rate constant. The scalar rate constants arise from (1) intrinsic relaxation processes of the radical which exist in the absence of the other paramagnetic site and (2) a scalar-exchange-induced relaxation process arising from orbital overlap between the two paramagnetic sites. The orientation-dependent rate constant arises from a dipole-dipole-induced relaxation process. From simulations of the higher temperature saturation-recovery transients, we conclude that their nonexponential character arises from a dipole-dipole interaction with the diferric center of RNR. The tyrosine radical generated by UV photolysis of L-tyrosine in a borate glass is used as a model for the intrinsic spin-lattice relaxation rate of the tyrosine radical of ribonucleotide reductase. Comparison of the scalar rate constants derived from simulations of the saturation-recovery transients of the tyrosine radical of RNR with the single-exponential rate constants of the model tyrosine radical indicates scalar exchange is also a source of relaxation enhancement of the tyrosine radical of RNR at higher temperatures. We present a new method for determining the exchange coupling of the diferric center based on the temperature dependence of the scalar-exchange and dipolar rate constants. The Fe(III)-Fe(III) exchange coupling is estimated to be $-94 \pm 7$ cm$^{-1}$. We also estimate an exchange coupling of $|0.0047 \pm 0.0003$ cm$^{-1}|$ between the diferric center and the tyrosine radical on the basis of the relative contributions of scalar-exchange and dipolar interactions to the spin-lattice relaxation and the distance between the two sites. The source of line broadening of the EPR signal of the tyrosine radical of RNR at temperatures greater than 75 K is discussed as well.

## Introduction

The enzyme ribonucleotide reductase (RNR) catalyzes the reduction of ribonucleotides to the corresponding deoxyribonucleotides. RNR from *Escherichia coli* consists of two subunits, B1 and B2, both of which are homodimers.[1] The B1 subunit binds the allosteric effectors and the substrate ribonucleotides, but both B1 and B2 contribute to the active site of the enzyme. Each polypeptide of the B2 subunit of RNR from *E. coli* contains one non-heme $\mu$-oxo-$\mu$-carboxylato-bridged dinuclear Fe(III) com-

[†] Yale University.
[‡] Current address: Department of Chemistry, Vanderbilt University, Nashville, TN 37235.
[§] University of Minnesota.

(1) Atkin, C. L.; Thelander, L.; Reichard, P.; Lang, G. *J. Biol. Chem.* **1973**, *248*, 7464-7472.

0002-7863/92/1514-7475$03.00/0 

plex[1-5] and a tyrosine residue at position 122. Tyrosine 122 is the site of a neutral[6,7] tyrosyl radical,[8-12] which has been shown to be essential for activity of the enzyme.[13] Ashley and Stubbe[14] have suggested that the tyrosyl radical plays a role in the abstraction of a hydrogen atom from the 3′ position of the substrate ribonucleotide. However, the X-ray crystal structure recently solved by Nordlund et al.[5] indicates that tyrosine 122 is approximately 10 Å from the protein surface, making it unlikely that this radical is directly responsible for hydrogen atom abstraction. The diferric center appears to stabilize the tyrosine residue in its radical state through an unknown mechanism. Mixing of the apoprotein with Fe(II) in the presence of oxygen results in the simultaneous formation of the diferric center and the tyrosyl radical.[1,4,15,16]

In an electron paramagnetic resonance (EPR) study of the magnetic interaction between the tyrosyl radical and the diferric center, Sahlin et al.[11] employed the conventional continuous-wave (CW) progressive power saturation technique to study the relaxation of the tyrosyl radical in the B2 subunit of RNR from *E. coli* and from a mammalian source. For the *E. coli* B2 subunit, they showed that the presence of the adjacent diferric center dramatically enhances the relaxation of the tyrosyl radical as the temperature is raised above 28 K. It was also noted that EPR signals from *E. coli* RNR broadened at temperatures greater than 75 K. The relaxation enhancement was attributed primarily to the presence of a magnetic dipolar interaction between the tyrosyl radical and the diferric center. However, the separate contributions of magnetic dipole–dipole and scalar-exchange interactions to the relaxation enhancement could not be assessed, since the CW method they employed measures only the overall magnitude of relaxation rate enhancement.

In this and earlier work by our group,[17] we have sought to measure pairwise dipole–dipole and scalar-exchange interactions by measuring the enhancement each interaction provided to spin–lattice relaxation. However, measurement of electron spin–lattice relaxation rates in a rigid matrix (frozen solution) is complicated by the fact that the inhomogeneous line width is always greater than the pulse width. Under these conditions, saturation–recovery and spin echo are "hole burning" experiments, since only a fraction of the spin packets which make up the signal can be saturated or given a 180° pulse. In addition to spin–lattice relaxation, there are two processes which can "fill in the hole" and hence contribute to the observed recovery: spectral diffusion and cross relaxation. Spectral diffusion occurs when spins outside the hole move into the hole (resonant field position) because of changes in the electron–nuclear hyperfine, dipolar, or quadrupolar couplings. Dalton and co-workers[18,19] have shown in saturation–recovery experiments on radicals in frozen matrices that long saturating pulses suppress spectral diffusion. In a study by Beck et al.,[20] it was demonstrated that long saturating pulses suppress the contributions of spectral diffusion to the spin–lattice relaxation of the tyrosine radical of RNR at low temperatures. Near liquid helium temperatures, it was found that as the length of the saturating pulse approached the characteristic recovery time, the observed $T_1$'s converged to a longer, essentially constant, value and the saturation–recovery transients were well fit by a single exponential.

Cross relaxation occurs when the spin–spin interaction of two radicals in close proximity causes a mutual "spin flip". This process enhances the observed relaxation rate when one of the spins is in the hole (resonant field position) and the other is outside the hole. The rate of cross relaxation is distance dependent. For a frozen solution of radicals, one expects that its contribution to the observed relaxation rate will be nonexponential, since each radical will have a different distribution of radicals around it. We also expect that, in the limit of very high dilution, cross relaxation will not contribute significantly to the observed relaxation. Apparently, the matrix of UV-generated tyrosine radicals used in this work and in our previous studies[17,20] comes close to meeting this criterion, since in the limit of long saturating pulses the saturation–recovery transients are well fit by a single exponential. (The concentration of tyrosine radicals is approximately 50 μM.[11]) For the stable tyrosine radical of RNR, one would expect little if any cross relaxation, since the protein surrounding the radicals prevents their close approach and the protein concentration is also low.

We have shown in earlier work[17] that the pulsed EPR method of saturation–recovery[21] allows one to determine the contributions of both dipolar and scalar-exchange interactions to the spin–lattice relaxation. If spectral diffusion and cross relaxation are suppressed, the saturation–recovery transient directly reflects the recovery of the bulk $z$-magnetization of the observed spins. For magnetically isolated spins, one expects that the bulk $z$-magnetization will recover with single-exponential kinetics. If, however, a dipole–dipole interaction enhances the relaxation of the observed spins with a rate constant that is a function of that spin's orientation and the spins are in a fixed but random orientation within the sample, then the saturation–recovery transient will be the *superposition* of many single-exponential recoveries. The net result is a non-single-exponential recovery for the bulk magnetization. The equations we have developed allow us to separate the contribution of the orientation-dependent (dipolar) relaxation enhancement from the isotropic relaxation. Given a suitable model for the unperturbed (intrinsic) relaxation of the observed spin, we can evaluate the relative contributions that the intrinsic relaxation rate and the scalar-exchange relaxation rate make to the isotropic relaxation.

As discussed earlier, we found that photochemically generated and cryogenically trapped tyrosyl radicals in a borate glass behave as magnetically isolated spins; i.e., they show single-exponential spin–lattice relaxation kinetics.[17] In the same study, we demonstrated that the saturation–recovery transient is non-single-exponential for the electron spin–lattice relaxation of the stable tyrosyl radical $Y_D^\bullet$ in photosystem II. The nonexponentiality of the transients was attributed to a dipolar interaction of $Y_D^\bullet$ with the non-heme Fe(II) in Mn-depleted PSII preparations. On the basis of a comparison of the isotropic or "scalar" spin–lattice relaxation of $Y_D^\bullet$ with that of the UV-generated tyrosyl radical, we concluded that there is no detectable exchange coupling between $Y_D^\bullet$ and the non-heme Fe(II).

We have probed the interaction between the tyrosyl radical and the diferric center of the B2 subunit of RNR isolated from *E. coli* using the pulsed EPR method of saturation–recovery. In these

(2) Petersson, L.; Gräslund, A.; Ehrenberg, A.; Sjöberg, B.-M.; Reichard, P. *J. Biol. Chem.* **1980**, *255*, 6706–6712.
(3) Sjöberg, B.-M.; Loehr, T. M.; Sanders-Loehr, J. *Biochemistry* **1982**, *21*, 96–102.
(4) Lynch, J. B.; Juarez-Garcia, C.; Münck, E.; Que, L., Jr. *J. Biol. Chem.* **1989**, *264*, 8091–8096.
(5) Nordlund, P.; Sjöberg, B.-M.; Eklund, H. *Nature* **1990**, *345*, 593–598.
(6) Backes, G.; Sahlin, M.; Sjöberg, B.-M.; Loehr, T. M.; Sanders-Loehr, J. *Biochemistry* **1989**, *28*, 1923–1929.
(7) Bender, C. J.; Sahlin, M.; Babcock, G. T.; Barry, B. A.; Chandrashekar, T. K.; Salowe, S. P.; Stubbe, J.; Lindström, B.; Petersson, L.; Ehrenberg, A.; Sjöberg, B.-M. *J. Am. Chem. Soc.* **1989**, *111*, 8076–8083.
(8) Gräslund, A.; Sahlin, M.; Sjöberg, B.-M. *Environ. Health Perspect.* **1985**, *64*, 139–148.
(9) Thelander, L.; Reichard, P. *Annu. Rev. Biochem.* **1979**, *48*, 133–158.
(10) Sjöberg, B.-M.; Gräslund, A. *Adv. Inorg. Biochem.* **1983**, *5*, 87–110.
(11) Sahlin, M.; Petersson, L.; Gräslund, G.; Ehrenberg, A.; Sjöberg, B.-M.; Thelander, L. *Biochemistry* **1987**, *26*, 5541–5548.
(12) Stubbe, J. A. *Annu. Rev. Biochem.* **1989**, *58*, 257–285.
(13) Thelander, L. *J. Biol. Chem.* **1974**, *249*, 4858–4862.
(14) Ashley, G. W.; Stubbe, J. *Pharmocol. Ther.* **1985**, *30*, 301–329.
(15) Ellasson, R.; Jörnvall, H.; Reichard, P. *Proc. Natl. Acad. Sci. U.S.A.* **1986**, *83*, 2373–2377.
(16) Bollinger, J. M., Jr.; Edmondson, D. E.; Huynh, B. H.; Filley, J.; Norton, J. R.; Stubbe, J. *Science* **1991**, *253*, 292–298.
(17) Hirsh, D. J.; Beck, W. F.; Innes, J. B.; Brudvig, G. W. *Biochemistry* **1992**, *31*, 532–541.
(18) Dalton, L. R.; Kwiram, A. L.; Cowen, J. A. *Chem. Phys. Lett.* **1972**, *17*, 495.
(19) Dalton, L. R.; Kwiram, A. L.; Cowen, J. A. *Chem. Phys. Lett.* **1972**, *14*, 77.
(20) Beck, W. F.; Innes, J. B.; Lynch, J. B.; Brudvig, G. W. *J. Magn. Reson.* **1991**, *91*, 12–29.
(21) Hyde, J. S. In *Time-Domain Electron Spin Resonance*; Kevan, L., Schwartz, R. N., Eds.; John Wiley & Sons: New York, 1979; pp 1–30.

experiments the $z$-magnetization of the "slow"-relaxing spin, the tyrosyl radical at Tyr 122, was saturated and its recovery was analyzed to determine if the neighboring "fast"-relaxing spin, the antiferromagnetically exchange-coupled diferric center, perturbed it. UV-generated tyrosyl radicals in a borate glass were employed as a model for the intrinsic relaxation of the tyrosyl radical in RNR. At low temperatures the spin–lattice relaxation rates and temperature dependence of the UV-generated tyrosyl radical closely parallel those of the tyrosyl radical in RNR. However, the high-temperature data indicate that there is a magnetic interaction between the tyrosyl radical and diferric center in the B2 subunit of RNR which involves both magnetic dipolar and scalar-exchange interactions. Petersson et al.[2] determined that the (antiferromagnetic) exchange coupling of the diferric center is $J_{ex} = -108^{+25}_{-20}$ cm$^{-1}$ ($\mathcal{H} = -2J_{ex}(\vec{S}_1 \cdot \vec{S}_2)$) by static magnetic susceptibility measurements on the B2 subunit. A new method is presented for determining the exchange coupling between the Fe(III)'s of the diferric center using the temperature dependence of the scalar and dipolar rates of the tyrosyl radical. It is also demonstrated that when there is a significant enhancement of the spin–lattice relaxation of the slow-relaxing spin due to scalar exchange with the fast-relaxing spin, it is possible to determine the magnitude of the exchange coupling between the slow and fast relaxers.

## Experimental Section

**Sample Preparation.** *E. coli* N6405/pSPS2, a strain that overproduces the B2 subunit of RNR, was obtained as a gift from Professor Joanne Stubbe and Scott P. Salowe and was grown as previously described.[22] The B2 subunit was purified as previously described[20] and had a specific activity of 5000, 3.8 Fe ions per B2 subunit, and 1.4 tyrosine radicals per B2 subunit, in agreement with published results.[4] The 300-$\mu$L EPR sample contained approximately 240 $\mu$M tyrosyl radical, 50 mM HEPES, pH 7.6, and 20% (v/v) glycerol and was stored in liquid nitrogen.

L-Tyrosine was used as received from Aldrich. L-Tyrosyl radicals[11] were generated in a frozen solution of 10 mM L-tyrosine and 12.5 mM sodium borate, pH 10. The radicals were generated by an 8-min illumination with a 250-W Hg arc lamp at 77 K.

Saturation–recovery EPR spectroscopy and conventional continuous-wave (CW) EPR spectroscopy were performed on a home-built X-band pulsed EPR spectrometer.[20] Saturation–recovery transients were obtained with direct CW detection (without magnetic field or microwave frequency modulation) in the absorption mode as described previously.[17,20] Sample temperatures were controlled by an Oxford ESR-900 cryostat system. Sample temperatures were measured using a gold–chromel thermocouple held in a sample tube at the sample position.

The methodology for determining the scalar ($k_{1scalar}$), dipolar ($k_{1d}$), and single-exponential ($1/T_1$) rate constants has been described previously.[17] Fits to the temperature dependence of the relaxation rates in Figures 2–4 were found using Kaleidagraph (Abelbeck Software/Synergy Software), which employs a Marquardt algorithm.

## Theory

In order to describe the expected spin–lattice relaxation of the tyrosyl radical in ribonucleotide reductase, we assume that relaxation enhancement arises from the pairwise interaction of the slow-relaxing spin (the tyrosyl radical) with the fast-relaxing spin (the neighboring diferric center). Since the protein is in a frozen glass, for each pair of slow and fast relaxers the interspin (spin-to-spin) vector is in a fixed but random orientation with respect to the static magnetic field. The dipole–dipole-induced relaxation enhancement is a function of the angle $\theta$ between the interspin vector and the static magnetic field, and all orientations of the interspin vector between 0 and $\pi$ are possible. The saturation–recovery transient, which reflects the spin–lattice relaxation of all of the slow-relaxing spins, can then be described by the following equation[17]

$$I(t) = 1 - N\int_0^{\pi} (\sin\theta)(e^{-(k_{1scalar}+k_{1\theta})t})\, d\theta \qquad (1)$$

where $k_{1scalar}$ is the contribution of isotropic relaxation processes and $k_{1\theta}$ is the contribution of the orientation-dependent dipole–dipole interaction. We refer to eq 1 as the "dipolar model" for the spin–lattice relaxation of the slow-relaxing spin.

We assume that there are two contributions to the scalar rate constant; i.e.

$$k_{1scalar} = k_{1i} + k_{1ex} \qquad (2)$$

where $k_{1i}$ is the relaxation rate of the tyrosyl radical in the absence of the fast-relaxing spin, i.e. the "intrinsic" relaxation rate, and $k_{1ex}$ is the relaxation rate due to scalar exchange. The form of the equation describing the intrinsic spin–lattice relaxation rate depends on the mechanism(s) of relaxation. We find that the temperature dependence of the spin–lattice relaxation rate ($1/T_1$) of the UV-generated tyrosyl radical is best fit by assuming a Raman relaxation mechanism which gives an equation of the form $1/T_1 = AT^n$, where $A$ is the spin–phonon coupling constant and $n$ is a function of the density of vibrational states (phonons) in the lattice.

The spin–lattice relaxation rate due to scalar exchange depends on the properties of both the fast- and slow-relaxing spins and is given by

$$k_{1ex} = \frac{2(J_{ex}(Fe_2\text{–}Y))^2\mu_{eff}^2}{3g_f^2\beta^2} \frac{1}{\omega_s^2(1 - g_f/g_s)^2 T_{2f}} \qquad (3)$$

where $J_{ex}(Fe_2\text{–}Y)$ is the exchange coupling between the fast (diferric center, $Fe_2$) and slow (tyrosyl radical, Y) relaxers, $\mu_{eff}^2$ is the effective magnetic moment of the fast-relaxing spin, $g_f$ and $g_s$ are the $g$ values for the fast and slow relaxers, respectively, $\beta$ is the Bohr magneton, $\omega_s$ is the resonant frequency of the slow-relaxing spin, and $T_{2f}$ is the transverse (spin–spin) relaxation time of the fast-relaxing spin.

The expression for the dipolar rate constant, $k_{1d}$, is also a function of the magnetic properties of both spins and is given by

$$k_{1\theta} = k_{1d}(1 - 3\cos^2\theta)^2 \qquad (4)$$

where

$$k_{1d} = \frac{\gamma_s^2\mu_{eff}^2}{6r^6} \frac{1}{\omega_s^2(1 - g_f/g_s)^2 T_{2f}} \qquad (5)$$

$\gamma_s$ is the magnetogyric ratio for the slow-relaxing spin, and $r$ is the interspin distance between the fast- and slow-relaxing spins. Equations 3–5 were derived[17] in the limit where $(g_s - g_f)^2 \ll g_s^2$, $(g_s + g_f)^2$ and, at X-band, in the limit where $T_{2f} \gg 10^{-11}$ s. Equations 4 and 5 were derived from the "$B$" term of the dipolar alphabet, which is expected to dominate the dipolar-induced relaxation in these limits.

All of the factors on the right-hand side of eqs 3 and 5 are assumed to be independent of temperature with the exception of $\mu_{eff}$ and $T_{2f}$. The effective magnetic dipole moment of the antiferromagnetically coupled diferric center is strongly temperature dependent. The general expression for $\mu_{eff}^2$ for an exchange-coupled dinuclear center is

$$\mu_{eff}^2 = g_f^2 \sum_S \frac{S(S+1)(2S+1)e^{-E(S)/kT}}{Z} \qquad (6)$$

where $Z = \sum_S (2S+1)e^{-E(S)/kT}$. $E(S)$ is the energy for a particular spin state, $S$. For antiferromagnetic exchange coupling, it is convenient to define the zero of energy such that $E(S) = -J_{ex}S(S+1)$, where $J_{ex}$ is the exchange coupling of the dinuclear center. In the present case, $J_{ex}$ is $J_{ex}$(Fe–Fe), the exchange coupling of the diferric center of RNR. $\mu_{eff}^2$ is in units of Bohr magnetons squared.

At low temperatures, where $J_{ex}(Fe\text{–}Fe) \gg kT$, only the ground $S = 0$ state will be populated and $\mu_{eff}^2$ will be zero. As the temperature is raised, the higher spin states become populated. For an exchange coupling of 108 cm$^{-1}$ and temperatures under 77 K, only the $S = 0$ and $S = 1$ spin states are significantly populated and $\mu_{eff}^2$ can be approximated by the expression

(22) Salowe, S. P.; Stubbe, J. *J. Bacteriol.* **1986**, *165*, 363–366.

$$\mu_{\text{eff}}^2 = g_f^2(6e^{2J_{ex}(\text{Fe-Fe})/kT}) \quad (7)$$

Using eq 7 rather than eq 6 gives less than 1% error in $\mu_{\text{eff}}^2$ for the temperatures and exchange coupling quoted above.

In the case where *only* $\mu_{\text{eff}}$ is a function of temperature, $k_{1ex}$ and $k_{1d}$ will have the same temperature dependence, since both are proportional to $\mu_{\text{eff}}^2$. In addition, the temperature dependence of $k_{1ex}$ and $k_{1d}$ will directly reflect the exchange coupling between the two Fe(III)'s of the diferric center. Equations 3, 5, and 7 predict that a plot of ln ($k_{1ex}$) or ln ($k_{1d}$) vs $1/T$ will have a slope of $2J_{ex}(\text{Fe-Fe})/k$.

$T_{2f}$, the transverse relaxation time of the diferric center, may or may not be a function of temperature. $T_2$ is normally considered to be independent of temperature for spins trapped in a rigid lattice. However, there are two other correlation times which place an upper limit on $T_{2f}$ and which are expected to be a function of temperature. The diferric center can enhance the relaxation of the tyrosyl radical only while in the excited $S = 1$ spin state (ignoring for now higher spin states). The lifetime of the excited $S = 1$ spin state, $\tau_1$, puts an upper limit on $T_{2f}$, i.e. $\tau_1 \geq T_{2f}$. Hence, if $\tau_1$ is sufficiently short, $T_{2f}$ will show the same temperature dependence as $\tau_1$. The same considerations apply to $T_{1f}$. Since $T_{1f} \geq T_{2f}$, if $T_{1f}$ is sufficiently short, $T_{2f}$ will show the same temperature dependence as $T_{1f}$.

If $T_{2f}$ *is* temperature dependent, eqs 3 and 5 still predict that $k_{1ex}$ and $k_{1d}$ will show the same temperature dependence, since both are proportional to $\mu_{\text{eff}}^2/T_{2f}$. Furthermore, regardless of whether $T_{2f}$ is or is not temperature dependent, eqs 3 and 5 can be used to determine the magnitude of the exchange coupling between the diferric center and the tyrosyl radical if the distance between them is known. Taking the ratio of $k_{1ex}$ to $k_{1d}$ and solving for $J_{ex}(\text{Fe}_2\text{-Y})$, we find

$$|J_{ex}(\text{Fe}_2\text{-Y})| = \sqrt{\frac{\beta^2 g_f^2 \gamma_s^2}{4r^6} \frac{k_{1ex}}{k_{1d}}} \quad (8)$$

Scalar-exchange and dipolar interactions can also enhance the transverse relaxation of the slow-relaxing spin ($T_{2s}$). This can be measured directly by the spin-echo technique or indirectly by line broadening of the CW EPR signal. The transverse relaxation rate constant for scalar exchange is given by

$$k_{2ex} = \frac{(J_{ex}(\text{Fe}_2\text{-Y}))^2 \mu_{\text{eff}}^2}{g_f^2 \beta_2}\left[\frac{1}{3}\left(T_{1f} + \frac{T_{2f}}{1 + \omega_s^2(1 - g_f/g_s)^2 T_{2f}^2}\right)\right] \quad (9)$$

and the relaxation rate constant for the dipole–dipole interaction is given by

$$k_{2\theta} = k_{2d}(1 - 3\cos^2\theta)^2 \quad (10)$$

where

$$k_{2d} = \frac{\gamma_s^2 \mu_{\text{eff}}^2}{3r^6} T_{1f} \quad (11)$$

Again, we have assumed[17] that $T_{1f}$, $T_{2f} \gg 10^{-11}$ s. Hence, the "*A*" term of the dipolar alphabet, expressed in eqs 10 and 11, dominates the expression.

## Results

**Fit of the Dipolar Model to Spin–Lattice Relaxation of the RNR Tyrosyl Radical.** Saturation–recovery transients were collected over a temperature range of 4.7–72 K. Figure 1a shows a saturation–recovery trace of the tyrosyl radical of the B2 subunit of ribonucleotide reductase at 56 K and the best fit of the dipolar model. Curves b and c of Figure 1 are the residual traces for the dipolar model and a single-exponential fit, respectively.

**Temperature Dependence of Spin–Lattice Relaxation.** Figure 2 presents the rate constants $k_{1\text{scalar}}$ and $k_{1d}$ vs temperature for the tyrosyl radical of the RNR B2 subunit. In the low-temperature regime, which is defined below, the rate constant for a single-exponential fit to the same saturation–recovery transients is also

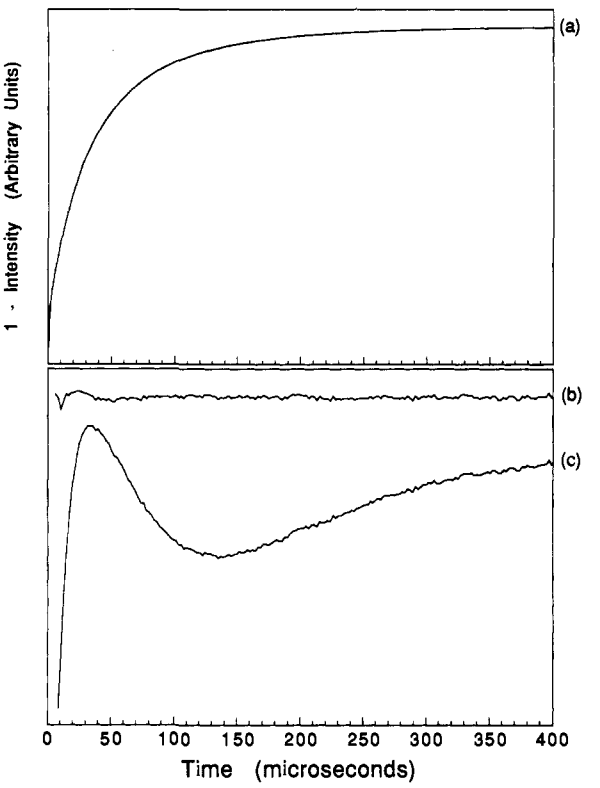


**Figure 1.** (a) Saturation–recovery transient obtained for the tyrosyl radical of the B2 subunit of ribonucleotide reductase with the fit by the dipolar model (eq 1) superimposed. The observing microwave power level was 23 $\mu$W, and the saturating microwave pulse (450 mW) was of 100-$\mu$s duration. The magnetic field was set at the low-field crossing point of the CW EPR signal of the tyrosyl radical for this transient and for all the saturation–recovery transients analyzed for Figure 2. The time between the end of the saturating pulse and the start of the fit to the transient is 6 $\mu$s. The residuals (the differences between the saturation–recovery transients and the fitted curves) for (b) the dipolar model and (c) a single exponential are plotted on an expanded vertical scale using the same scaling factor for both.

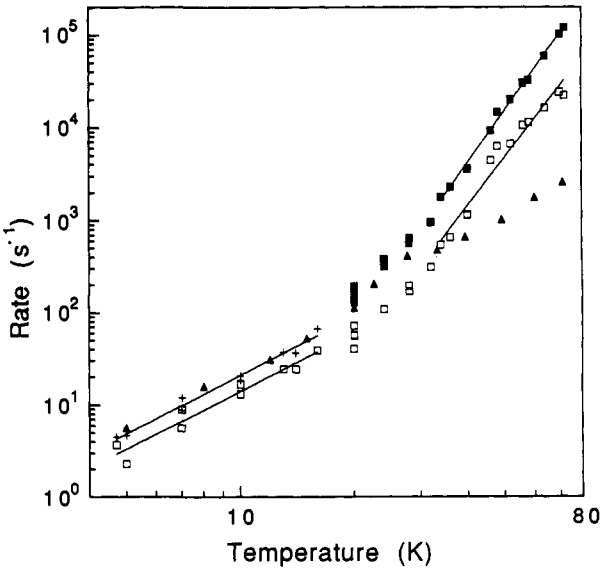


**Figure 2.** Scalar, dipolar, and single-exponential electron spin relaxation rate constants ($k_{1\text{scalar}}$ (□), $k_{1d}$ (■), and $1/T_1$ (+), respectively) for the tyrosyl radical of the B2 subunit of ribonucleotide reductase obtained as a function of sample temperature. $k_{1\text{scalar}}$ and $k_{1d}$ were obtained by fitting the dipolar model to the saturation–recovery transients at each temperature. $1/T_1$ was found by fitting a single exponential to the saturation–recovery transients at each temperature. The single-exponential ($1/T_1$) spin–lattice relaxation rates for the UV-generated tyrosyl radical (▲) are plotted in order to allow comparison with the values of $k_{1\text{scalar}}$ and $1/T_1$ of ribonucleotide reductase.

shown. The single-exponential rate constants for the UV-generated tyrosyl radical, our model for $k_{1i}$, have been included for comparison.

For our analysis and for comparison of our results to those of Sahlin et al.,[11] we divide the relaxation rate data of Figure 2 into three regimes. The low-temperature regime is defined by 4.7 K $\leq T \leq$ 16 K. In this regime, the saturation–recovery transients are essentially single exponential. When saturation–recovery transients in this temperature regime were fit by the dipolar model, $k_{1d}$ (not shown) was found to be less than or approximately equal to the scalar rate constant, $k_{1scalar}$. Calculations of $\mu_{eff}^2$ based on $J_{ex}$(Fe–Fe) = −108 cm$^{-1}$ indicate that it should be too small at these temperatures to produce any detectable scalar-exchange or dipolar relaxation of the tyrosyl radical. Hence, $k_{1scalar} = k_{1i}$, and $k_{1d}$ is expected to be zero. That the fitted value of $k_{1d}$ is not strictly zero in these data sets is mainly a reflection of the difficulty of eliminating all low-frequency noise components in this experiment.

The high-temperature regime is defined by 34 K $\leq T \leq$ 72 K. In this regime $k_{1d}$ is consistently greater than $k_{1scalar}$, approximately by a factor of 3. By 34 K, $k_{1scalar}$ of the tyrosyl radical in the B2 subunit of RNR has "crossed over" the single-exponential rate constant $(1/T_1)$ of the UV-generated tyrosyl radical. The difference between these two rate constants increases sharply in this temperature range. The scalar rate constant clearly has a steeper temperature dependence in the high-temperature regime than it does in the low-temperature regime. The latter two observations indicate that in this regime the contribution of scalar-exchange-induced relaxation to $k_{1scalar}$ is much greater than that of intrinsic relaxation; i.e., $k_{1scalar} \simeq k_{1ex}$.

The midtemperature regime is defined as 16 K $< T <$ 34 K. In this regime the contributions of $k_{1ex}$ and $k_{1i}$ to the scalar rate constant, $k_{1scalar}$, are comparable in magnitude.

Comparison of our relaxation rate constants with the progressive power saturation data of Sahlin et al.[11] reveals the same trends although the transition from the low-temperature regime to the high-temperature regime appears to be more gradual in our data set. Sahlin et al.[11] defined their low-temperature regime as 10 K $< T \leq$ 28 K. In this regime they found that the temperature dependence of the relaxation rate product, $(T_1T_2)^{-1}$, of the tyrosyl radical of RNR was well fit by the power law equation $(T_1T_2)^{-1} = AT^{2.0}$, where $A$ is a constant and $T$ is the temperature in Kelvin. We find essentially the same temperature dependence for the scalar (obtained from a fit to eq 1) and single-exponential rate constants of the tyrosyl radical of RNR. In our low-temperature regime, 4.7 K $\leq T \leq$ 16 K, we find that $k_{1scalar}$ is well fit by the power law equation $k_{1scalar} = (0.12 \pm 0.02)T^{2.1\pm0.2}$. The power law dependence of the single-exponential fit to the same data is $(1/T_1) = (0.17 \pm 0.02)T^{2.1\pm0.1}$ (Figure 2).

In the low-temperature regime, Sahlin et al.[11] found that the temperature dependence of the spin–lattice relaxation of the UV-generated tyrosyl radical closely paralleled that of ribonucleotide reductase. They found that the relaxation rate product for the UV-generated tyrosyl radical could be fit well over the entire temperature range, 10 K $< T <$ 77 K, by the equation $(T_1T_2)^{-1} = BT^{2.0}$, where $B = A$ to within the experimental error of their measurements. We found in our earlier experiments on the UV-generated tyrosyl radical that over the 5–70 K temperature range the best fit was given by $(1/T_1) = 0.11T^{2.4}$. However, if we restrict our fit of the model tyrosyl data to the low-temperature regime, i.e. 4.7 K $\leq T \leq$ 16 K, we find that the optimal fit is $(1/T_1) = (0.24 \pm 0.03)T^{2.0\pm0.1}$ (not shown). To within the uncertainty in the fits, this is the same temperature dependence determined for $k_{1scalar}$ and $1/T_1$ for the tyrosyl radical in ribonucleotide reductase. We believe, therefore, that the UV-generated tyrosyl radical is also a good model for the intrinsic spin–lattice relaxation rate, $k_{1i}$, of the tyrosyl radical of RNR.

In the high-temperature regime, 28 K $< T <$ 77 K, Sahlin et al.[11] found that the temperature dependence of the relaxation rate product was well fit by $(T_1T_2)^{-1} = CT^{5.7}$, where $C$ is a constant different from $A$. In our high-temperature regime, 34 K $\leq T \leq$ 72 K, we observe essentially the same temperature dependence as Sahlin et al.[11] for both $k_{1scalar}$ and $k_{1d}$. Power law fits to $k_{1scalar}$ vs temperature and $k_{1d}$ vs temperature yield $k_{1scalar} = ((4.8 \pm 0.5) \times 10^{-6})T^{5.3\pm0.3}$ and $k_{1d} = ((2.8 \pm 0.1) \times 10^{-6})T^{5.7\pm0.1}$ (Figure 2). The exponents for the fits of $k_{1scalar}$ and $k_{1d}$ are equal to each other to within the uncertainty of the fits.

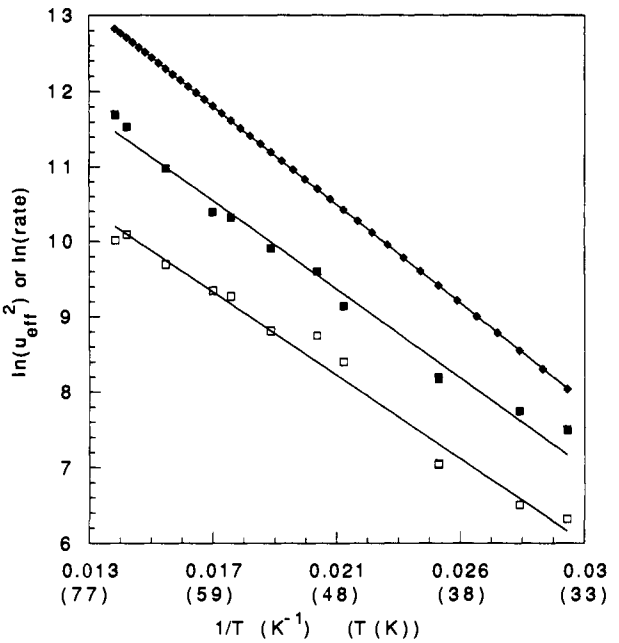


**Figure 3.** Natural logarithms of $k_{1scalar}$ (□), $k_{1d}$ (■), and $\mu_{eff}^2C$ (♦) versus $1/T$ using the high-temperature-regime data, 34 K $\leq T \leq$ 72 K, of Figure 2. $C$ is an arbitrary constant which changes only the $y$-intercept.

**Determination of the Exchange Coupling for the Diferric Center.** We noted in the theory section of this paper that if the temperature dependence of $k_{1ex}$ and $k_{1d}$ were due exclusively to the temperature dependence of $\mu_{eff}^2$, then the slope of a plot of ln $(k_{1ex})$ or ln $(k_{1d})$ vs $1/T$ should be equal to $2J_{ex}$(Fe–Fe)$/k$. Figure 2 suggests that, in the high-temperature regime, the scalar relaxation of the tyrosyl radical of RNR is dominated by relaxation due to scalar exchange. Therefore, one can replace $k_{1ex}$ by $k_{1scalar}$ in this temperature range. Figure 3 shows a plot of ln $(k_{1scalar})$ and ln $(k_{1d})$ vs $1/T$ for the high-temperature-regime data and the calculated curve ln $(\mu_{eff}^2)$ vs $1/T$ for the same temperature regime. The $y$-intercept of the ln $(\mu_{eff}^2)$ vs $1/T$ curve has been arbitrarily shifted so that the slopes of the lines can more easily be compared.

The slope of the ln$(\mu_{eff}^2)$ vs $1/T$ curve in Figure 3 corresponds to a $J_{ex}$(Fe–Fe) of −108 cm$^{-1}$, the exchange coupling determined by the static magnetic measurements of Petersson et al.[2] The slopes of the curves for ln $(k_{1scalar})$ and ln $(k_{1d})$ vs $1/T$ are equal to within experimental error, as predicted from eqs 3, 5, and 7. It is clear from Figure 3 that the slopes of the curves for ln $(k_{1scalar})$ and ln $(k_{1d})$ vs $1/T$ are slightly less than that of the ln $(\mu_{eff}^2)$ vs $1/T$ plot. However, the corresponding values of $J_{ex}$(Fe–Fe) determined from the $k_{1scalar}$ and $k_{1d}$ data, 91 ± 4 cm$^{-1}$ and 97 ± 4 cm$^{-1}$, respectively, fall within the experimental uncertainty of the exchange coupling determined by Petersson et al.[2], i.e. $J_{ex} = -108^{+25}_{-20}$ cm$^{-1}$. Taking the average of our two values for $J_{ex}$(Fe–Fe) and the total uncertainty, we find that $J_{ex}$(Fe–Fe) = −94 ± 7 cm$^{-1}$.

**An Equation for $k_{1scalar}$.** If we are correct in assuming that, in the low-temperature regime, $k_{1scalar} = k_{1i}$ and that, in the high-temperature regime, $k_{1scalar} = k_{1ex}$, we can now construct an equation for $k_{1scalar}$ based on eq 2 which should describe its temperature dependence over the entire temperature range of 4.7 K $\leq T \leq$ 72 K, i.e.

$$k_{1scalar} = (0.11T^{2.1}) + ((1.2 \times 10^{-6})e^{2(94/kT)}) \qquad (12)$$

In eq 12 we have used the average value of $J_{ex}$(Fe–Fe) determined from $k_{1scalar}$ and $k_{1d}$. The preexponential factor of the second term in eq 12 is the result of fitting the data for ln $(k_{1scalar})$ vs $1/T$ in Figure 3 with $J_{ex}$(Fe–Fe) fixed at −94 cm$^{-1}$. Equation 12 is shown superimposed on a plot of $k_{1scalar}$ vs $T$ in Figure 4. This equation produces a smooth curve through all the points, including those

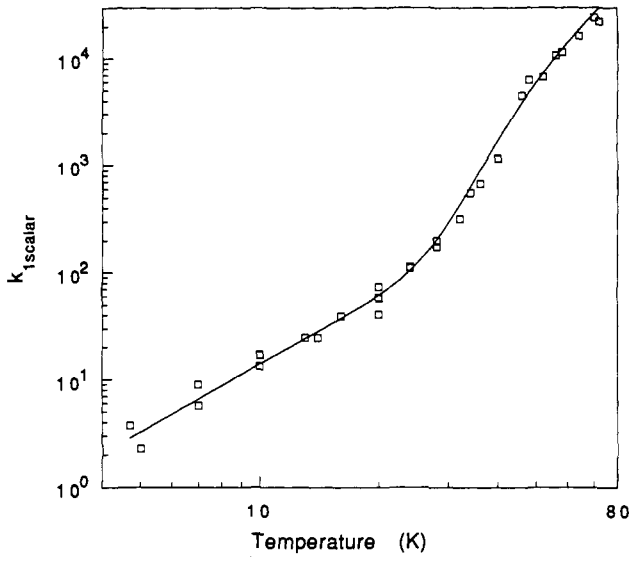


**Figure 4.** Scalar rate constant $k_{1scalar}$ (□) vs temperature with eq 12 superimposed.

in the midtemperature regime. If we fit all of the data points to the equation $k_{1scalar} = (AT^B) + (Ce^{-2D/kT})$, we obtain $k_{1scalar} = (0.12T^{2.1}) + ((1.3 \times 10^{-6})e^{2(97/kT)})$, which is the same as eq 12 to within the uncertainty in $A$, $B$, $C$, and $D$.

**Determination of the Diferric Center–Tyrosyl Radical Exchange Coupling.** We can estimate the exchange coupling between the diferric center and the tyrosyl radical using eq 8. We assume that $\gamma_s = \gamma_e$ and that $g_f = 2.00$. (Since the Fe(III)'s which make up the diferric center are high spin, there should be little spin–orbit coupling to shift the $g$-value from its free electron value.) From our high-temperature-regime data, we have $k_{1ex}/k_{1d} = k_{1scalar}/k_{1d} = 0.326 \pm 0.042$. Equation 8 treats the slow- and fast-relaxing paramagnetic centers as point dipoles. We take the distance $r$ to be the distance between the geometric centers of spin density of the fast and slow relaxers. Hence, $r$ is the distance from the center of the diferric center to the center of the phenyl ring of the tyrosyl radical. From the crystallographic coordinates,[23] we find that $r = 8.71$ Å. Equation 8 then yields $|J_{ex}(Fe_2\text{–}Y)| = 141 \pm 9$ MHz or $0.0047 \pm 0.0003$ cm$^{-1}$ where the uncertainty in the exchange coupling assumes that the point dipole approximation is valid.

**Source of Line Broadening at Temperatures > 75 K.** Sahlin et al.[11] observed line broadening of the EPR signal from *E. coli* ribonucleotide reductase at temperatures above approximately 75 K. Since the line width of the model tyrosyl radical is invariant up to 150 K, the increase in line width is presumably not due to intrinsic relaxation processes. Therefore, the question arises as to whether the increase in line width is due to the dipole–dipole or scalar-exchange interactions of the tyrosyl radical with the diferric center, or both. We assume that the increase in line width of the tyrosyl radical EPR signal is due to broadening of the individual Lorentzian spin packets that make up the line shape. Their broadening in turn is due to changes in $T_2$ of the tyrosyl radical; for a Lorentzian line shape, the half-width at half-height is given by $1/(\pi T_2)$. The transverse relaxation enhancement provided by scalar exchange is given by eq 9, and the dipolar relaxation enhancement is given by eqs 10 and 11. The relative relaxation enhancement provided by the dipolar and scalar-exchange interactions can be expressed as the ratio $k_{2\theta}/k_{2ex}$. If we assume that $T_{1f} \gg T_{2f}/[1 + \omega_2^2(1 - g_f/g_s)^2 T_{2f}^2]$, then we can write eq 9 as

$$k_{2ex} = \frac{(J_{ex}(Fe_2\text{–}Y))^2 \mu_{eff}^2}{g_f^2 \beta^2} \frac{T_{1f}}{3} \qquad (13)$$

and the ratio $k_{2\theta}/k_{2ex}$ is simply

$$\frac{k_{2\theta}}{k_{2ex}} = \frac{\gamma_s^2 \beta^2 g_f^2}{(J_{ex}(Fe_2\text{–}Y))^2 r^6}(1 - 3\cos^2\theta)^2 \qquad (14)$$

The average value of $(1 - 3\cos^2\theta)^2$ is $^2/_3$. Substitution into eq 14 yields $\langle k_{2\theta}/k_{2ex} \rangle \simeq 8$, indicating that the dipolar interaction is the primary source of line broadening for the *E. coli* RNR tyrosyl radical.

## Discussion

As Figure 1 illustrates, a single exponential is inadequate to describe the spin–lattice relaxation of the tyrosyl radical in the high-temperature regime, while the dipolar model provides a good fit to the data. One might ask whether the nonexponential character of the saturation–recovery traces arises from the orientation dependence of a *pairwise* dipolar interaction or the distance dependence of dipolar interactions between the tyrosyl radical and *several* paramagnetic centers. We can consider the interaction between the tyrosyl radical and the diferric center of each polypeptide of the B2 homodimer to be pairwise so long as the dipolar and scalar-exchange interactions between them are much greater than those between the tyrosyl radical and any other paramagnetic centers within or outside each B2 subunit. The structure of the B2 subunit makes this a reasonable assumption. While the center-to-center distance between the tyrosyl radical and the diferric center of each polypeptide is only 8.71 Å,[23] the two diferric centers of the B2 subunit are 25 Å apart.[5] Interenzyme paramagnetic interactions are likely to be weak, since each protein molecule is "far" from the next at the protein concentrations used in these experiments and, even if there were protein–protein "association", Tyr 122 is buried 10 Å from the protein surface.[5] For the same reason, paramagnetic interactions between the tyrosyl radical and extraneous metal ions are unlikely to be the source of the nonexponentiality in the spin–lattice relaxation transients.

The temperature dependence of the spin–lattice relaxation rate constants observed by saturation–recovery closely parallels the temperature dependence of the relaxation rate product observed by Sahlin et al.[11] Both the high- and low-temperature-regime data indicate that the temperature dependence of the relaxation rate product observed by Sahlin et al.[11] is due largely, if not exclusively, to changes in $T_1$ of the tyrosyl radical of RNR ($T_{1s}$). For the temperature regime 4.7 K $\leq T \leq$ 72 K, we confirm that $T_2$ of the tyrosyl radical ($T_{2s}$) is essentially temperature independent, an assumption often made when interpreting the results of CW EPR progressive power saturation experiments.

One might ask why $T_{2s}$ is temperature independent, when the same scalar-exchange and dipolar interactions that enhance spin–lattice relaxation also enhance transverse relaxation. The answer is that relaxation enhancement due to scalar-exchange and dipolar interactions is apparent only if this enhancement is large compared to the intrinsic spin–lattice or intrinsic transverse relaxation. Since the spins are in a rigid glass throughout this temperature regime, we can assume that the intrinsic transverse rate is fixed at the rigid lattice limit. We can crudely estimate the intrinsic transverse relaxation rate ($k_{2i}$) by assuming that the Lorentzian spin packets that comprise the Gaussian-shaped EPR signal have a line width of 1 G. This gives $k_{2i} \simeq 9 \times 10^6$ s$^{-1}$. Using the UV-generated tyrosyl radical as a model for the intrinsic spin–lattice relaxation, Figure 2 indicates that, even at 70 K, $k_{1i}$ is only on the order of $3 \times 10^3$ s$^{-1}$. Hence, the spin–lattice relaxation rate is much more sensitive to perturbations from scalar-exchange and dipolar interactions.

While at higher temperatures, $T > 75$ K, Sahlin et al.[11] observed no line broadening in the EPR signal from the UV-generated tyrosine radical, line broadening was observed in the EPR signal from the tyrosyl radical of RNR. At this temperature, relaxation enhancement from magnetic interactions with the diferric center has apparently "caught up" with the intrinsic transverse relaxation of the radical. We attribute the line broadening primarily to enhancement of the transverse relaxation rate of the tyrosyl radical ($T_{2s}$) by its dipolar interaction with the diferric center. We note that the dipolar enhancement of the transverse relaxation rate

(23) Ecklund, H.; Sjöberg, B.-M. Private communication.

could be direct, i.e. occurring through the process described by eqs 10 and 11, or indirect, i.e. $T_2$ of the tyrosyl radical becoming limited by $T_1$ if spin–lattice relaxation becomes sufficiently fast. In either case, dipolar relaxation enhancement is expected to be the primary source of line broadening although the relative contributions of scalar-exchange relaxation enhancement will differ for the direct and indirect processes.

Our experimental determination of $J_{ex}$(Fe–Fe) = $-94 \pm 7$ cm$^{-1}$ is valid only if $T_{2f}$ is *not* a function of temperature. We can make the following arguments against a significant temperature dependence for $T_{2f}$. Assume for the moment that both $\mu_{eff}^2$ and $T_{2f}$ are temperature dependent. Then, in the high-temperature regime

$$\ln (k_{1ex}) = \ln (k_{1scalar}) = \ln (A) + \ln (\mu_{eff}^2) + \ln (1/T_{2f}) \quad (15)$$

and

$$\ln (k_{1d}) = \ln (B) + \ln (\mu_{eff}^2) + \ln (1/T_{2f}) \quad (16)$$

where $A$ and $B$ represent the temperature-independent terms in eqs 3 and 5, respectively. $1/T_{2f}$ will increase with increasing temperature. If $1/T_{2f} \propto e^{-\Delta/kT}$, i.e. if relaxation were due to an Orbach-type mechanism in the limit where $\Delta > kT$, it is clear from eqs 15 and 16 that the effect of this on a plot of ln ($k_{1scalar}$) or ln ($k_{1d}$) vs $1/T$ would be to simply *increase* the observed slope by $\Delta$ and, hence, the apparent magnitude of $J_{ex}$(Fe–Fe) by $\Delta/2$. What if the temperature dependence of $1/T_{2f}$ were due to a Raman relaxation mechanism, i.e. $1/T_{2f} \propto T^n$? We have simulated the effect of such a temperature dependence on a plot of ln ($\mu_{eff}^2$) vs $1/T$ with the assumption that $J_{ex}$(Fe–Fe) = $-108$ cm$^{-1}$ and $n = 2$. The power law temperature dependence of $1/T_{2f}$ introduces some curvature in the plot, but what is more apparent is the increase in slope. When a straight line is fit to the points, the magnitude of the apparent exchange coupling increases by 33 cm$^{-1}$, even with this fairly weak temperature dependence. (If $n = 1$, the magnitude of the apparent exchange coupling increases by 16 cm$^{-1}$.) Either an exponential or power law temperature dependence for $1/T_{2f}$ would increase the apparent value of $J_{ex}$(Fe–Fe), and yet our value of $|J_{ex}$(Fe–Fe)| is near the *lower* limit of the exchange coupling determined by Petersson et al.[2] Therefore, we conclude that $T_{2f}$ is essentially independent of temperature below 72 K.

Other researchers have formulated equations similar to ours to describe the relaxation enhancement due to scalar-exchange and dipole–dipole interactions; but these equations have employed $T_{1f}$ as the relevant correlation time, or the authors have tacitly assumed that $T_{2f} = T_{1f}$. Our determination of $J_{ex}$(Fe–Fe) underscores the importance of choosing $T_{2f}$ as the relevant correlation time for determining the spin–lattice relaxation enhancement due to scalar-exchange and dipole–dipole interactions. If the relevant correlation time in eqs 3 and 5 were $T_{1f}$, we could not have determined $J_{ex}$(Fe–Fe), since undoubtedly the spin–lattice relaxation of the diferric center is strongly temperature dependent. Our finding that the transverse relaxation time of the diferric center ($T_{2f}$) is essentially independent of temperature is not surprising. Since the spins are in a rigid glass throughout this temperature regime, the intrinsic transverse relaxation rate is fixed at the rigid lattice limit. So long as $\tau_1$ and $T_{1f}$ are greater than $T_{2f}$, $T_{2f}$ can remain invariant. We found in our study of the stable tyrosyl radical of PSII that $T_{2f}$ *was* a function of temperature. In this instance we believe that $T_{2f}$ is limited by $T_{1f}$, i.e. $T_{1f} = T_{2f}$, because of the extremely fast spin–lattice relaxation. Using the equations of Calvo et al.,[24] we estimated that at 5 K $1/T_{1f} = 1.8 \times 10^7$ s$^{-1}$, which is faster than the transverse relaxation rate we estimate for the rigid lattice limit.

Using the temperature dependence of $k_{1d}$ or $k_{1ex}$ of a nearby radical to determine the exchange coupling of an adjacent dinuclear center may yield a more accurate value for the exchange coupling than static magnetic susceptibility measurements. The saturation–recovery method has the advantage that it is independent of the sample (radical) concentration and it requires no corrections for the diamagnetic susceptibility of the sample or the concentration of paramagnetic impurities.

We have assumed that there are only three contributions to spin–lattice relaxation of the tyrosyl radical. Figure 4 suggests that we are correct in assuming that only "intrinsic" and scalar-exchange relaxation processes contribute to the isotropic component of the spin–lattice relaxation. However, given the close proximity of the two spins, one might ask whether we should also have included anisotropic exchange coupling as a contribution to the orientation-dependent rate constant. Since the orientation-dependent contribution to relaxation is still approximately 3 times greater than the isotropic contribution and since the exchange coupling between the diferric center and the tyrosyl radical is very small, we believe that the contribution from anisotropic exchange is negligible.

The small exchange coupling between the diferric center and the tyrosyl radical ($|J_{ex}(Fe_2–Y)| = 0.0043 \pm 0.0003$ cm$^{-1}$) may not seem surprising in light of what is known about the two paramagnetic centers. Sahlin et al.[11] produced an *E. coli* B2 subunit with deuterated tyrosine, L-[3,5-$^2$H]tyrosine, at the radical site and $^{57}$Fe(III) at the diferric center and yet found no evidence for a hyperfine interaction between the deuterated tyrosyl radical and the dinuclear $^{57}$Fe(III) site.[11] Also, the crystal structure shows that Tyr 122 lies outside the first coordination sphere of the diferric center.[5] On the other hand, in bacterial reaction centers from *Rhodobacter sphaeroides*, there is a relatively strong exchange interaction between the non-heme Fe(II) and the adjacent semiquinone, $Q_A^-$.[25] $Q_A$ lies outside the first coordination sphere of non-heme Fe(II) and at approximately the same distance from the iron "center" as Tyr 122 in ribonucleotide reductase,[5,26] yet the exchange coupling is almost 100 times greater.[25] Hydrogen bonding between one of the histidine residues coordinated to the Fe(II), His M219, and $Q_A^-$ may account for the enhancement in the exchange coupling between these two sites in the bacterial reaction center. The crystal structure of the bacterial reaction center[26] and CW EPR spectra of the Fe(II)–$Q_A^-$ and Fe(II)–$Q_B^-$ states of the reaction center indicate that there is hydrogen bonding between $Q_A^-$ and His M219. However, it appears from the crystallographic coordinates of the B2 subunit of RNR that there is no opportunity for hydrogen bonding between Tyr 122 and any of the residues coordinated to the diferric center. Resonance Raman[6] and ENDOR[7] experiments have established that the tyrosine radical at Tyr 122 is deprotonated. One could imagine that the tyrosyl radical is a weak hydrogen-bond acceptor, but there is no ligand on the diferric center which is a potential hydrogen-bond donor and is sufficiently close to the tyrosyl radical to form a hydrogen bond.[23]

**Acknowledgment.** The crystallographic coordinates of Tyr 122 and the dinuclear Fe(III) complex were kindly provided by Professors Hans Eklund and Britt-Marie Sjöberg. This work was supported by NSF Grant DMB 9104669 (L.Q.) and NIH Grant GM 36442 (G.W.B.).

(24) Calvo, R.; Butler, W. F.; Isaacson, R. A.; Okamura, M. Y.; Fredkin, D. R.; Feher, G. *Biophys. J.* **1982**, *37*, 111a.

(25) Butler, W. F.; Calvo, R.; Fredkin, D. R.; Isaacson, R. A.; Okamura, M. Y.; Feher, G. *Biophys. J.* **1984**, *45*, 947–973.

(26) Allen, J. P.; Feher, G.; Yeates, T. O.; Komiya, H.; Rees, D. C. *Proc. Natl. Acad. Sci. U.S.A.* **1988**, *85*, 8487–8491.